

AD-A279 450

It is estimated to average 1 hour per response, including the time for reviewing instructions, searching existing data sources, gathering and reviewing the collection of information. Send comments regarding this burden estimate or any other aspect of this collection of information, including this burden estimate, to Washington Headquarters Services, Directorate for Information Operations and Reports, 1215 Jefferson Avenue, Washington, DC 20540, and to the Office of Management and Budget, Paperwork Reduction Project (0714-0188), Washington, DC 20503.

2. REPORT DATE
13 May 1994**3. REPORT TYPE AND DATES COVERED**
Technical 6/93-5/94**4. TITLE AND SUBTITLE**Surface Second Harmonic Studies of Si(111)/Electrolyte and Si(111)/SiO₂/Electrolyte Interfaces**5. FUNDING NUMBERS**

ONR N00014089-J-1261

R&T Code 4131038

6. AUTHOR(S)

P. R. Fischer, J. L. Daschbach and G. L. Richmond

7. PERFORMING ORGANIZATION NAME(S) AND ADDRESS(ES)Department of Chemistry
1253 University of Oregon
Eugene, OR 97403**8. PERFORMING ORGANIZATION REPORT NUMBER**

ONR Technical Report

#9

9. SPONSORING/MONITORING AGENCY NAME(S) AND ADDRESS(ES)Office of Naval Research Attn: Dr. Peter Schmidt
Chemistry Program
800 North Quincy St.
Arlington, VA 22217-5000**10. SPONSORING/MONITORING AGENCY REPORT NUMBER**DTIC
ELEC
MAY 19 1994**11. SUPPLEMENTARY NOTES****12a. DISTRIBUTION/AVAILABILITY STATEMENT**

Approved for public release: distribution unlimited

12b. DISTRIBUTION CODE**13. ABSTRACT (Maximum 200 words)**

The optical second harmonic (SH) response from Si(111) electrode surfaces has been studied and has been found to be highly potential dependent. For both H-terminated Si(111) surfaces in NJ₄F, and oxide covered surfaces biased in H₂SO₄, the phase and the amplitude display a potential dependence which we attribute to field effects within the semiconductor space-charge region and at the surface of the Si(111) electrode. The studies are the first to demonstrate that for Si(111)/oxide samples, the potential dependence in the SH phase can be correlated with oxide thickness, as demonstrated by examining samples of 0-40 Angstrom thickness.

94-15029

94 5 105

14. SUBJECT TERMS

Si(111)/oxide electrodes; electrochemistry

15. NUMBER OF PAGES
15**16. PRICE CODE****17. SECURITY CLASSIFICATION OF REPORT**
Unclassified**18. SECURITY CLASSIFICATION OF THIS PAGE**
Unclassified**19. SECURITY CLASSIFICATION OF ABSTRACT**
Unclassified**20. LIMITATION OF ABSTRACT**

OFFICE OF NAVAL RESEARCH

Grant N00014-89-J-1261

R&T Code 4131038

Technical Report no. 9

**"Surface Second Harmonic Studies of Si(111)/Electrolyte and
Si(111)/SiO₂/Electrolyte Interfaces"**

by

P.R. Fischer, J.L. Daschbach, and G. L. Richmond

Submitted to Chemical Physics Letters

**Department of Chemistry
1253 University of Oregon
Eugene, OR 97403**

May 1994

Reproduction in whole, or in part, is permitted for any purpose of the United States Government.

This document has been approved for public release and sale; its distribution is unlimited.

**SURFACE SECOND HARMONIC STUDIES OF Si(111)/ELECTROLYTE AND
Si(111)/SiO₂/ELECTROLYTE INTERFACES**

1

P. R. Fischer, J. L. Daschbach and G.L. Richmond


Dept. of Chemistry
University of Oregon
Eugene, OR 97403

Abstract:

The optical second harmonic (SH) response from Si(111) electrode surfaces has been studied and has been found to be highly potential dependent. For both H-terminated Si(111) surfaces in NH₄F, and oxide covered surfaces biased in H₂SO₄, the phase and the amplitude display a potential dependence which we attribute to field effects within the semiconductor space-charge region and at the surface of the Si(111) electrode. The studies are the first to demonstrate that for Si(111)/oxide samples, the potential dependence in the SH phase can be correlated with oxide thickness, as demonstrated by examining samples of 0-40 Å thickness.

*Submitted to
Chemical Physics Letters
9/15/93*

Accepted 12/93

Accession For	
NTIS GRA&I	<input checked="checked" type="checkbox"/>
DTIC TAB	<input type="checkbox"/>
Unannounced	<input type="checkbox"/>
Justification	
By	
Distribution/Avail	
Availability Codes	
Dist	Avail and/or Special
A-1	

Although Si/electrolyte and Si/SiO₂/electrolyte interfaces have been extensively investigated, many issues regarding the structural, electronic and electrochemical properties of these interfaces remain of interest. Understanding the nature of these interfaces has much technological relevance. In recent years significant progress has been made in characterizing the Si/electrolyte interface with FT-IR experiments,^{1, 2} UHV transfer experiments,³ and STM^{4, 5, 6, 7} and AFM⁸ imaging by taking advantage of the relative stability of Si surfaces prepared in a hydrogen terminated state. However, these probes are inapplicable for measuring the Si/SiO₂ interface once several overlayers of SiO₂ are present. In this letter we report the results of the first surface second harmonic generation (SHG) study which explicitly probes the properties of the Si/SiO₂ electrolyte interface as a function of oxide thickness. The results are compared with the potential dependent response for H-terminated Si surfaces. Because of the inherent surface sensitivity of SHG, it is a useful probe of interfacial regions, particularly buried interfaces which are difficult to probe by other techniques.⁹ Although SHG and sum frequency generation (SFG) have been used in many studies to examine Si(111) in UHV^{10, 11} and in air,^{12, 13} application to Si/electrolyte and Si/SiO₂/electrolyte interfaces have been almost nonexistent. Of the two earlier electrochemical studies reported in this area,^{14, 15} both were performed prior to recent advances in surface preparation procedures and neither have involved the polarization and surface orientation experiments necessary to understand the origin of the potential dependent response as has been done here.

The most striking result is the strong potential dependence that we observe in the relative phase of the SH response, as measured with rotational anisotropy experiments,¹⁶ from both the H-terminated surfaces and surfaces with oxides. We attribute the potential dependence for both the predominately H-terminated and the oxide covered surface to the change in the static field at the surface and within the space-charge region (SCR) of the semiconductor. In the presence of the insulating oxide layer, the potential dependence can be interpreted in terms of a screening of the portion of the applied dc field. The work

demonstrates that such phase measurements provide a new means of characterizing the properties of the space charge region and the field drop across the insulating oxide layer. The ability to observe potential dependence and its origin has been questionable up to this point because of the relatively large bulk response from semiconductors. A recent report has investigated the effect of the depletion layer electric field on the SHG response from GaAs(001) under UHV conditions but this study was limited to a smaller range of electric fields than reported here and was performed only on native surfaces.¹⁷

II. THEORETICAL CONSIDERATIONS

When a potential is applied across a semiconductor/electrolyte interface, the second harmonic response can be written as

$$I_{SH} \propto || \vec{F} (\tilde{\chi}_B^{(2)} + \tilde{\chi}_S^{(2)} + \tilde{\chi}_{eff}^{(3)} \Delta\Phi) ||^2 \quad (1)$$

where \vec{F} corresponds to the linear Fresnel factors, $\tilde{\chi}_S^{(2)}$ and $\tilde{\chi}_B^{(2)}$ are the surface and bulk susceptibilities, $\tilde{\chi}_{eff}^{(3)} \Delta\Phi$ is the effective cubic nonlinearity arising from the static field which includes all terms that vary linearly with field strength.¹⁸ $\Delta\Phi$ is the potential drop across the semiconductor space charge region and is proportional to the difference between the applied (E_{app}) and the flatband (E_{fb}) potential. When the SH response is dominated by the cubic nonlinearity term, the observed potential dependence should be parabolic with a minimum near the flatband potential. Such behavior has been observed in numerous studies of metal/electrolyte systems. Under conditions where the surface and/or bulk quadratic nonlinearities dominate, parabolic potential dependence with a minimum shifted from flatband would be observed.

By judicious choice of input and output polarizations, and by monitoring the variation in the SH response as the cubic sample is rotated azimuthally, a detailed analysis of the relative contribution from the various tensor elements, χ_{ijk} , can be performed.¹³ The observed angular variation (rotational anisotropy) can be related to the overall symmetry of the surface atomic structure. The intensity of this azimuthal dependence for a

(111) surface and the input and output polarizations used here can be described by the phenomenological equations¹⁹

$$I(2\omega)_{p,p} \propto |a^{(\infty)} + c^{(3)}\cos(3\phi)|^2 \quad (2)$$

$$I(2\omega)_{p,s} \propto |b^{(3)}\sin(3\phi)|^2 \quad (3)$$

where the azimuthal angle ϕ is defined as the angle between the $[2\bar{1}\bar{1}]$ direction and the projection of the incident wavevector parallel to the surface. The subscripts p and s denote the beam polarizations for the fundamental and second harmonic respectively. The isotropic coefficient $a^{(\infty)}$, and the anisotropic coefficients, $b^{(3)}$ and $c^{(3)}$, contain both the Fresnel coefficients as well as the material susceptibility elements. The isotropic coefficient, often discussed as the out-of-plane response, contains the three independent surface tensor elements χ_{xx} , χ_{yy} , and χ_{zz} ($i=x,y$) as well as the bulk elements ζ and γ . The anisotropic coefficients contain the in-plane χ_{xx} surface tensor element and bulk element ζ . Because the experiments conducted under both p-input and output polarizations (Eq. 2) involve an interference between $a^{(\infty)}$ and $c^{(3)}$ the fits to the data provide information about the relative magnitude and phase of these two terms. For the potential dependent measurements, $\chi_{ijkl}^{(3)}$ has the same form as $\chi_{ijk}^{(2)}$ as a result of the applied field being parallel to the surface normal about which the sample is rotated.

III. EXPERIMENTAL METHODS

The optical measurements employ the fundamental output from a 10 Hz Nd:YAG laser producing 10 nsec pulses which illuminate the surface at a 32° incident angle. Pulses of ≈ 0.3 J/cm² were used which is below the damage threshold for silicon. The optics, detection instrumentation and electrochemical cell are similar to that described previously.²⁰ The silicon wafers are n-doped with phosphorus with a resistivity of 3.0 to 6.5 Ω -cm which represents a defect doping density of $\approx 10^{15}$ cm⁻³. The 0.66-0.71 mm thick samples are degreased by ultrasonification in separate baths of methylene chloride, acetone, and methanol and dried with nitrogen. The back of the wafer is etched for one minute in 48% hydrofluoric acid to remove the native oxide and then mounted on Ga-In

eutectic that has been placed on an embedded copper contact in a Kel-F shaft. A mask containing an embedded acid resistant fluorocarbon o-ring is used to seal the surface from the electrolyte.

The silicon wafer is prepared by etching in buffered NH_4F solution which is known to leave the surface in a H-terminated state.² This is followed by immersion in 0.1 M NH_4F if a hydrogen terminated surface is to be maintained, or in 0.1 M H_2SO_4 if an oxide is to be grown. Oxides are grown on the Si samples photoanodically by the stepwise increase in potential from the flatband to a final potential of +5.0 V while keeping the anodic current below $30\mu\text{A}/\text{cm}^2$. A HeNe laser is used for illumination. Thicknesses of the oxides are determined by a combination of ellipsometry, photocurrent measurements, and etch-back times. All potentials are referenced to the saturated calomel electrode (SCE). Flatband potentials are determined by photocurrent transients.

IV. RESULTS AND DISCUSSION

Figure 1 shows the rotational anisotropy in the SH response with p,p polarization for a Si(111) surface studied in NH_4F (Fig. 1(a)) and H_2SO_4 (Fig. 1(b)) at potentials near flatband, -0.65 V and -0.6 V respectively. Both samples were etched for 3 min. in 2.0 M NH_4F at pH 4.5 to produce a H-terminated surface prior to immersion. The three-fold symmetry expected of this (111) surface of a cubic lattice is observed in both solutions. The results for the surface in NH_4F gives a phase angle for $c^{(3)}/a^{(\infty)}$ of $25 \pm 5^\circ$. Previous studies suggest that this surface in NH_4F should remain predominately H-terminated when potentiostated near the flatband.²¹ It should also be relatively free of any photogenerated surface oxides since in fluoride containing electrolytes, the dissolution of this oxide should compete with the photo-oxidation process. The response from the same surface studied in H_2SO_4 is similar but the phase angle fluctuates between 30° - 60° . The flatband potential also varies slightly in time. We attribute both variations to photogenerated surface species which can store charge at the interface. From photocurrent measurements we estimate the amount of photogenerated species to be less than 3 ML.

The potential dependence of a Si(111) surface in 0.1 M NH_4F has been examined between -0.65 V (flatband) and +1.0 V. The experiments have been conducted at $\phi = 30^\circ$ so as to isolate the potential dependence in the isotropic and anisotropic contributions. As shown in Figure 2(a), both the isotropic and anisotropic response are found to have a parabolic potential dependence with a higher overall signal level from the latter. The isotropic response which would most readily couple to the applied static field has a minimum near +0.26 V, ≈ 900 mV from the flatband potential. This field can couple to a depth of the space charge region, which for this surface biased at +0.3 V is on the order of 1200 nm. The anisotropic in-plane response has a minimum near +1.6V, even further away from flatband. In H_2SO_4 the minima for the isotropic and anisotropic responses are also shifted from flatband.

The fact that the minimum signal does not occur at the flatband for the isotropic or anisotropic response in either solution suggests that terms other than $\tilde{\chi}_{\text{eff}}^{(3)} \Delta\Phi$ in Eq. 1 must be contributing. $\tilde{\chi}_B^{(2)}$ is the likely factor considering that the penetration depth of the light is on the order of 1 cm, considerably deeper than the SCR. Previous studies in air have determined that the SH contribution from the surface and the bulk of Si(111) are of similar magnitude.¹³ Further evidence for the importance of the bulk response comes from the observation that when Si(111) surfaces are roughened by etching in 48% HF prior to introduction into the NH_4F , the rotational anisotropies for the roughened and unroughened samples are quite similar. There is no evidence of an isotropic response from a disordered silicon surface superimposed on the response from the crystalline lattice. The intensity of the overall response is however slightly larger in the roughened case, suggesting that $\tilde{\chi}_s^{(2)}$ is not insignificant. Analysis of the response in Fig. 2(a) based on Eq. 1 indicates that the sum of $(\tilde{\chi}_s^{(2)} + \tilde{\chi}_B^{(2)})$ is at least of comparable magnitude to the contribution from $\tilde{\chi}_{\text{eff}}^{(3)} \Delta\Phi$.

In earlier work it was assumed that the electrode polarization was absolute with respect to zero applied potential (flatband) and a model of quadratic dependence of the SHG with applied potential was found to fit the data.¹⁵ Although the flatband was not

measured in these earlier studies, the current-voltage data presented suggests that the flatband potential was well negative of 0 V (vs. SCE). With this correction the data clearly do not fit a quadratic dependence in applied field strength but does resemble the data reported here.

In a similar manner the SH response has been studied for Si(111) surfaces for which varying thicknesses of SiO₂ have been photoanodically grown on the surface. Figure 3 shows the rotational anisotropy from an oxide covered surface in H₂SO₄ at two potentials, 0.0 V (Fig. 3(a)), the flatband potential at this oxide thickness, and +3.0V (Fig. 3(b)). The potential "window" for study of the oxide coated surfaces is wider due to the insulating nature of the overlayer. The oxide layer is estimated to be ≈ 25 Å based on etch back times²² and ellipsometry measurements. Because the electrochemically grown oxides have substantial water content in the first monolayers of oxide with this ratio decreasing as the thickness increases, we view our ellipsometrically determined thicknesses as an upper limit. In comparing the response from the Si(111) surfaces of Fig. 1(b) measured at flatband with the oxidized sample in Fig. 3(a), two important observations can be made. The rotational anisotropy persists in the presence of the oxide and the signal from the oxide covered surface is enhanced relative to the more oxide free sample in Fig. 1(b). The former observation is not surprising since the SH response from the amorphous oxide overlayer is very small.¹⁴ The signal enhancement observed in the presence of oxide demonstrates that the SHG is sensitive to the Si(111) surface adjacent to the oxide and is not merely a bulk response. This enhanced signal could be due to a crystalline interfacial region between the Si and the oxide overlayer as suggested in previous studies on thermal oxides.²³ It is more likely that the effect can be attributed to an interfacial strain in the Si lattice as has been observed in a strong resonant enhancement at SH photon energy of 3.3 eV and attributed to a direct transition taking place in a perpendicularly strained silicon layer at the thermal oxide Si/SiO₂ interface.²⁴ Comparison of thermal and anodic oxides will be reported elsewhere.

As with the Si(111) surfaces, there is a strong potential dependence in the response from the Si(111)/SiO₂ interface that is manifested in both the relative magnitude and phase of the rotational anisotropy (Compare Fig. 3(a) and 3(b)). For an applied field of +3.0 V beyond the flatband potential, which for this surface is 0.0 V, the relative phase angle between the anisotropic and isotropic response changes from 48° to 129°. The relative magnitude changes by a factor of two. The measured minima in the anisotropic and isotropic response occurs near +3.5V and +2.5 V respectively, both minima being far from the flatband potential. As with the Si(111) surfaces, the potential dependence for the oxidized surfaces does not follow the predicted form if $\tilde{\chi}_{eff}^{(3)} \Delta\Phi$ were the dominant factor.

To understand the strong potential dependence in the relative phase angle observed in Fig. 3 we have conducted rotational anisotropy experiments at a series of potentials for surfaces of different oxide thicknesses. A portion of the results are summarized in Table 1. Because the flatband potential varies with the oxide thickness, all data is referenced to the flatband potential of each sample as determined by photocurrent transient measurements. For all samples, the potential dependence follows the trend observed in Figure 3 for the 25 Å sample where the phase angle increases with increased positive potential. At flatband, the fits to the anisotropies for the different oxide covered samples show little variation as one would expect since $(\tilde{\chi}_s^{(2)} + \tilde{\chi}_B^{(2)})$ should be similar for samples with more than a few monolayers of SiO₂. The fact that the surface in NH₄F has a slightly different magnitude and phase (Fig. 1(a)) than the H₂SO₄ case is consistent with a different $\tilde{\chi}_s^{(2)}$ due to the presence of oxidized surface species. At potentials positive to flatband, a progressively larger V_{app} is necessary to achieve the magnitude of the phase angle that is obtained for surfaces with thinner oxide coatings. For example, the phase angles obtained for the 40 Å sample are shifted by approximately +1 V relative to the phase angles obtained from the 25 Å sample. We attribute the potential dependence in the phase angle to the variation of the field at the semiconductor surface and within the space charge region. Because of the insulating nature of the oxide, the field at the Si(111)/SiO₂ interface is no longer $\Delta\Phi$ but is reduced by the potential drop across the oxide layer, ΔV_{ox} .

This would suggest, for example, that the additional 15 \AA of oxide on the surface screens approximately 1V of the overall applied field relative to the 25 \AA sample. Later publications will address in more detail the correlation between phase and amplitude changes in the SH response with oxide thickness, doping density, and oxide composition.

In summary, SHG studies of hydrogen terminated Si(111) electrode surfaces and Si(111)/SiO₂ electrode surfaces of varied oxide thickness have been examined to determine the origin of the nonlinear response. The potential dependence from the initially prepared H-terminated surfaces in NH₄F suggests that the potential independent bulk response is significant in contrast to previous studies^{14, 15} which have described the response solely in terms of the field dependent third order term. For oxidized surfaces the response from the Si(111)/SiO₂ interfacial region is highly sensitive to the band bending conditions in the semiconductor and the insulating nature of the oxide overlayer. The studies show the sensitivity of SHG to the electrostatic properties of the Si/SiO₂ electrolyte interface and demonstrate the utility of extending this method to semiconductor electrode surfaces. Studies are underway to provide a more quantitative comparison between oxide properties and the potential dependent response for these surfaces.

Acknowledgments:

Funding from the National Science Foundation (CHE 8451346) is gratefully acknowledged.

Figure 1. Rotational anisotropy from Si(111) for p-input and p-output polarizations. (a) Si(111) in 0.1 M NH_4F biased at the flatband potential of -0.65 V. Best fit of Eq. 3 to the data yields $c^{(3)}/a^{(\infty)} = 2.2e^{i21^\circ}$; (b) Si(111) in 0.1 M H_2SO_4 biased at the flatband potential of -0.6 V; $c^{(3)}/a^{(\infty)} = 1.7e^{i44^\circ}$.

Figure 2. Potential dependence in the isotropic $a^{(\infty)}$ and anisotropic response $c^{(3)}$ for Si(111) prepared in a H-terminated state and biased in 0.1 M NH_4F . The isotropic response was monitored with p-polarized incident light and p-polarized SHG with $\phi = 30^\circ$. The anisotropic response was monitored with p-polarized incident light and s-polarized output light at $\phi = 30^\circ$.

Figure 3. Rotational anisotropy in the p-input and p-output SH response from an oxidized Si(111) sample in 0.1 M H_2SO_4 with approximately 25 Å of SiO_2 . (a) At 0.0 V (flatband), with $c^{(3)}/a^{(\infty)} = 2.3e^{i48^\circ}$; (b) At +3.0 V, $c^{(3)}/a^{(\infty)} = 4.7e^{i129^\circ}$.

Table 1: Fits to Rotational Anisotropy Data: $c^{(3)}/a^{(\infty)}$

$V_{\text{app}} - V_{\text{fb}}$	Oxide Thickness			
	$\approx 0 \text{ \AA} \text{ (H}_2\text{SO}_4\text{)}$	15 \AA	25 \AA	40 \AA
0 V (FB)	$1.8 e^{i50^\circ}$	$2.4 e^{i37^\circ}$	$2.3 e^{i48^\circ}$	$2.5 e^{i42^\circ}$
+0.5 V		$2.9 e^{i55^\circ}$	$2.8 e^{i61^\circ}$	$2.8 e^{i42^\circ}$
+1.0 V		$4.2 e^{i75^\circ}$	$3.4 e^{i72^\circ}$	$3.2 e^{i51^\circ}$
+1.5 V		$4.6 e^{i106^\circ}$	$4.0 e^{i89^\circ}$	$3.5 e^{i58^\circ}$
+2.0 V		$4.0 e^{i126^\circ}$	$5.0 e^{i113^\circ}$	$3.7 e^{i70^\circ}$
+2.5 V			$4.7 e^{i129^\circ}$	$4.5 e^{i92^\circ}$
+3.0 V				$5.1 e^{i110^\circ}$
+3.5 V				$4.8 e^{i120^\circ}$

1. P. Jakob, Y.J. Chabal, K. Ragahavachari, R.S. Becker and A.J. Becker, *Surface Science* **275** (1992) 407.
2. G.S. Higashi, Y.J. Chabal, G.W. Trucks and K. Raghavachari, *Appl. Phys. Lett.* **56** (1990) 656.
3. H.J. Lewerenz and T. Bitzer, *J. Electrochem. Soc.* **139** (1992) L21.
4. G.S. Higashi, R.S. Becker, Y.J. Chabal and A.J. Becker, *Appl. Phys. Lett.* **58** (1991) 1656.
5. H.E. Hessel, A. Feltz, M. Reiter, U. Memmert and R.J. Behm, *Chem. Phys. Lett.* **186** (1991) 275.
6. M. Szklarczyk, A. Gonzalez-Martin, O. Velez and J.O. Bockris, *Surface Science* **237** (1990) 305.
7. R. Houbertz, U. Memmert and R.J. Behm, *Appl. Phys. Lett.* **62** (1993) 2516.
8. Y. Kim and C.M. Lieber, *J. Am. Chem. Soc.* **113** (1991) 2333.
9. G.L. Richmond, J.M. Robinson and V.L. Shannon, *Prog. in Surf. Sci.* **28** (1988) 1.
10. T.F. Heinz, M.M.T. Loy and W.A. Thompson, *Phys. Rev. Lett.* **54** (1985) 63.
11. T.F. Heinz, M.M.T. Loy and W.A. Thompson, *J. Vac. Sci. Technol. B* **3** (1985) 1467.
12. H.W.K. Tom, T.F. Heinz and Y.R. Shen, *Phys. Rev. Lett.* **51** (1983) 1983.
13. H.W.K. Tom, *Ph.D. Dissertation* University of California, Berkeley, 1984.
14. O.A. Aktsipetrov and E.D. Mishina, *Phys. Dokl. Akad. Nauk SSSR* **274** (1984) 62.
15. C.H. Lee, R.K. Chang and N. Bloembergen, *Phys. Rev. Lett.* **18** (1967) 167.
16. H.W.K. Tom, T.F. Heinz and Y.R. Shen, *Phys. Rev. Lett.* **51** (1983) 1983.
17. J. Qi, M.S. Yeganeh, I. Koltov, A.G. Yodh and W.M. Theis, *Phys. Rev. Lett.* **71** (1993) 633.
18. P. Guyot-Sionnest and A. Tadjeddine, *J. Chem. Phys.* **92** (1990) 734.
19. J.E. Sipe, D.J. Moss and H.M. van Driel, *Phys. Rev. B* **35** (1987) 1129.
20. D.A. Koos, V.L. Shannon and G.L. Richmond, *J. Phys. Chem.* **94** (1990) 2091.
21. L.M. Peter, D.J. Blackwood and S. Pons, *J. Electroanal. Chem.* **294** (1990) 111.
22. H.J. Lewerenz, *Electrochim. Acta* **37** (1992) 847.
23. L.L. Kulyuk, D.A. Shutov, E.E. Strumban and O.A. Aktsipetrov, *J. Opt. Soc. Am. B: Opt. Phys.* **8** (1991) 1766.
24. W. Daum, H.-J. Krause, U. Reichel and H. Ibach, *Phys. Rev. Lett.* **71** (1993) 1234.

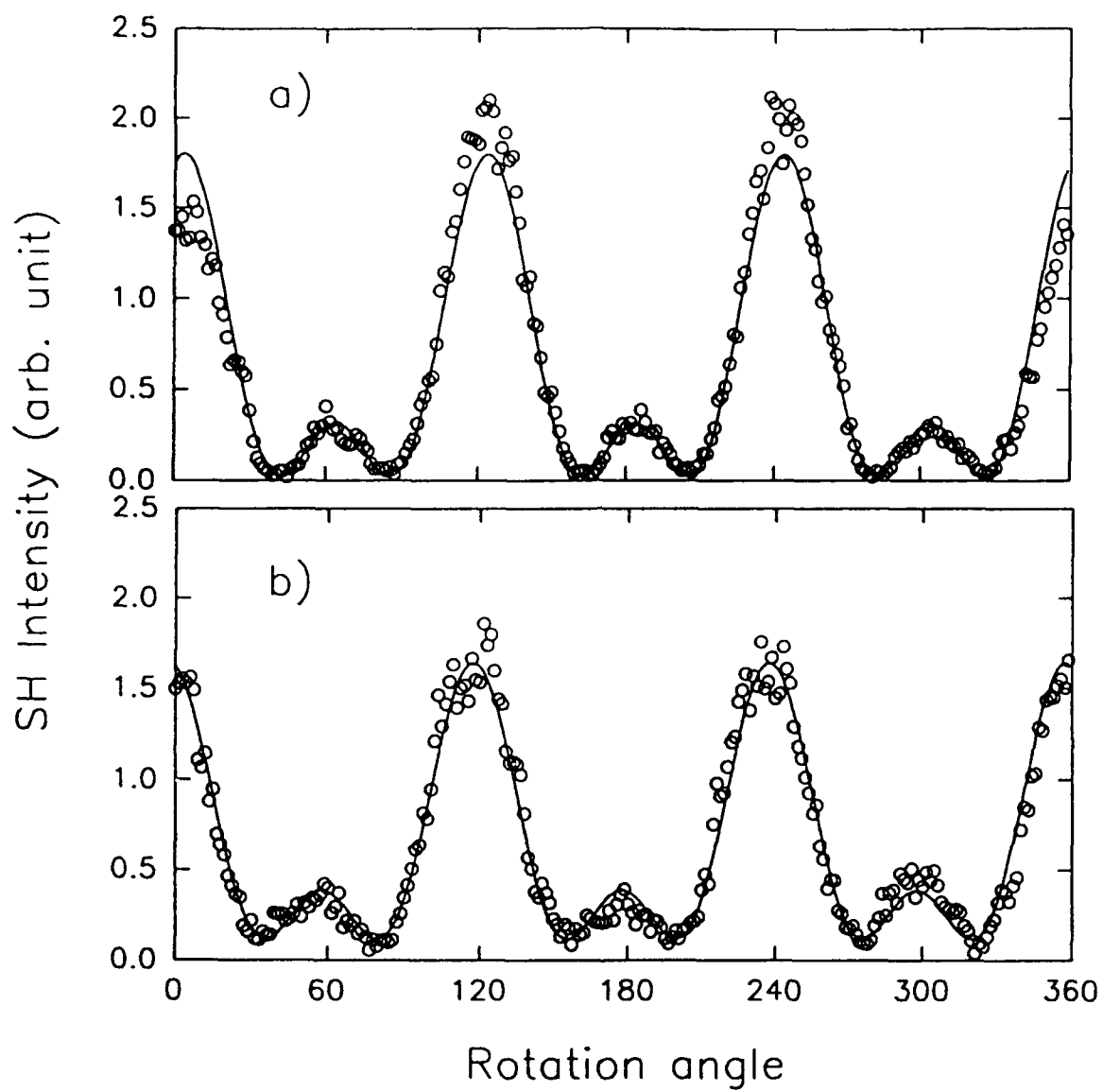


Fig 1.

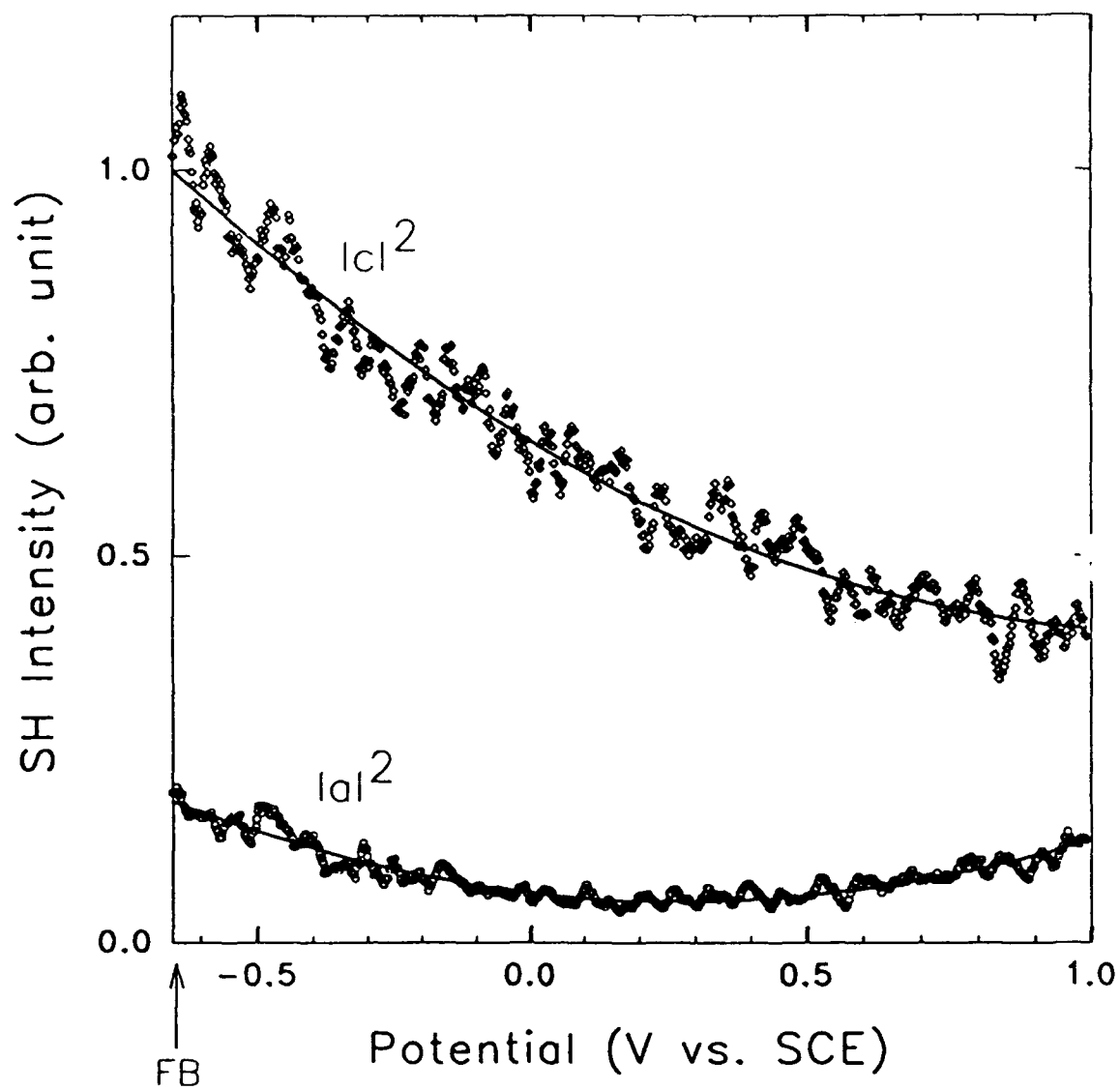


FIG. 2

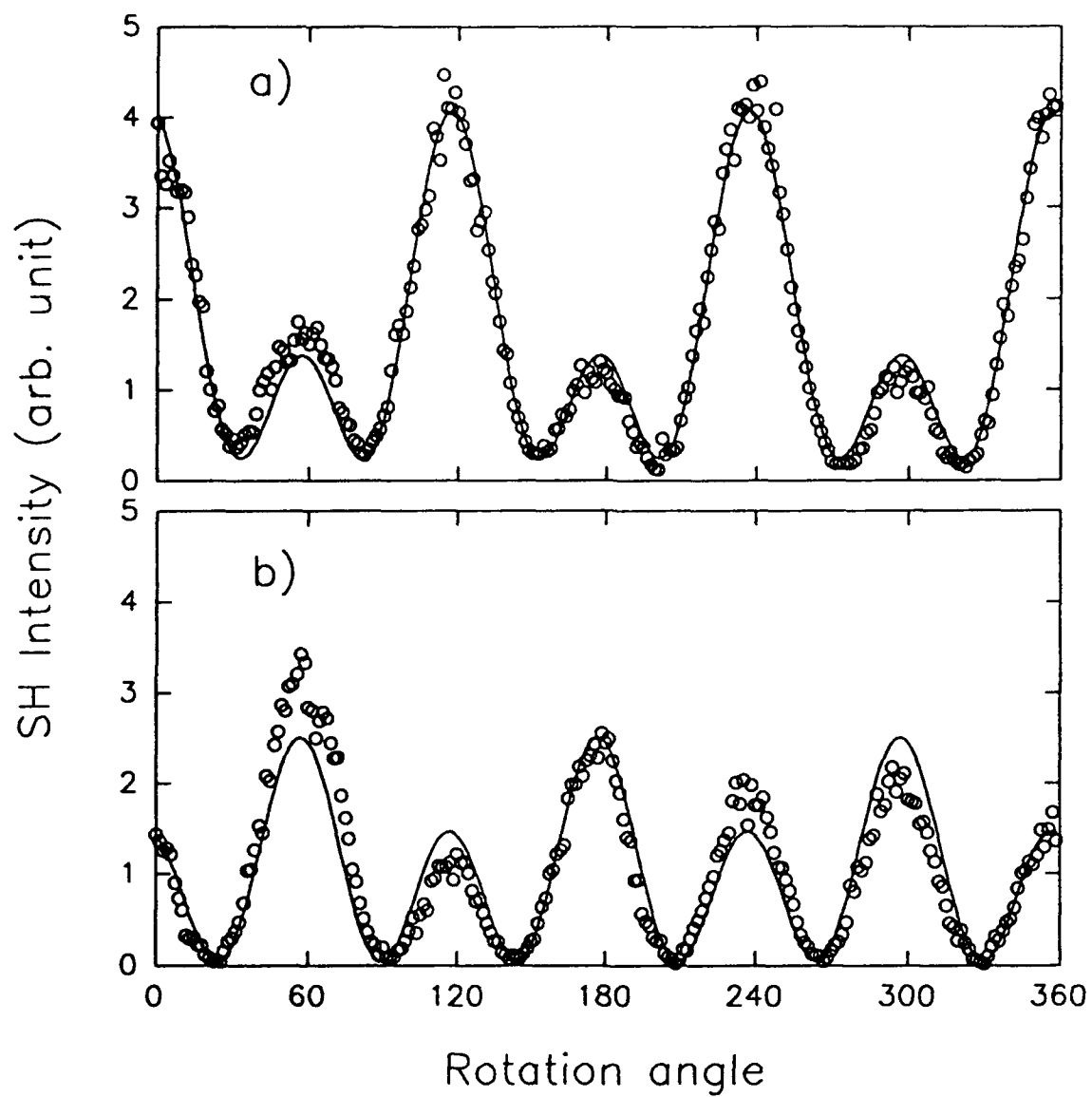


Fig. 3.